Scientia Iranica D (2018) 25(6), 3542–3558

Sharif University of Technology
Scientia Iranica
Transactions D: Computer Science & Engineering and Electrical Engineering
http://scientiairanica.sharif.edu

Design of a prototypical dual-axis tracker solar panel controlled by geared dc servomotors

A. Mansouri*, F. Krim, and Z. Khouni

Laboratory of Power Electronics and Industrial Control (LEPCI), Department of Electronics, Faculty of Technology, University Ferhat Abbas of SETIF1, El Maabouda, Route de Béjaia, Sétif 19000, Algeria.

Received 2 December 2015; received in revised form 27 November 2016; accepted 8 January 2018

KEYWORDS
Arduino Uno;
Dual axis;
Light-dependent resistor;
Low-cost solar tracker;
PWM control.

Abstract. The main challenges of solar tracking systems are sunlight sensing for maximum illumination, providing an initial position and delays of PV panel, and designing an adequate control unit for low-consumption servomotors. The objective of this paper is to design and implement an automatic control for directing maximum solar illumination to a photovoltaic (PV) panel. The proposed dual-axis solar tracker panel prototype is used to optimize the conversion of solar energy into electricity by orienting the panel toward the real position of the sun, at a cost of mechanical complexity and maintenance need, for the best efficiency. In hardware development, two geared dc servomotors are adjusted by Pulse Width Modulation (PWM) which is controlled by a drive unit moving the panel using four Light-Dependent Resistors (LDR) to provide analog signals; these signals are processed by a simple and low-energy ATMEGA328P microcontroller with Arduino. For the software part, after data processing, a C++ programming controls two dc servomotors to position light sensors in the most favorable direction, where solar panel and sensors can be perpendicular to the sunlight.

1. Introduction

Regarding the continuous depletion and pollution of resources by using fossil fuels (oil, natural gas, coal, etc.), thermonuclear (Uranium, plutonium, etc.), and the increasing demand for energy during the last forty years, researchers all over the world struggle to develop new technologies to produce clean, Renewable Electrical energy (REn) sources, such as solar and wind energy, to make them inexhaustible and accessible. Solar rays produced every day to our planet are million times greater than the consumption rate of the global electrical energy need. Solar energy is abundant, non-polluting, silent, reliable, free, and inexhaustible, needing very low maintenance. For this reason, solar energy will be widely used to produce clean electricity.

Solar trackers are devices that orient solar panels, Fresnel reflector, mirrors or lenses towards the sun to receive maximum radiation in the form of light and heat to be converted to thermal energy or produce electricity. In 1839, the French physicist Alexandre-Edmond Becquerel was the first researcher to discover that sunlight could be transformed into electricity. It is the photovoltaic (PV) effect. A century later, the first PV cells where constructed. The early solar modules were used in space in 1958. Other emerging technologies using multi-junction cells included concentrator photovoltaic (CPV) and Concentrated Solar Power (CSP), which must use trackers to be pointed at the sun; otherwise, no energy can be produced. For these reasons, researchers are interested in motorizing solar trackers. The main types of sun trackers are mechanical and electrical parts. In 1962, Finster

*. *Corresponding author. Tel.: +213 36 61 60 63*
E-mail address: mansouri51@yahoo.com (A. Mansouri)

doi: 10.24200/sci.2018.20045

introduced the first purely mechanical tracker [1]. In 1963, Saavedra designed an automatic electronic control mechanism [2]. Afterwards, several research works have been carried out on the design of single- and dual-axis solar tracking systems using electromechanical actuators to allow for about more produced energy (30% to 60%) as compared to the fixed system, because sunlight remains perpendicular to the PV panels [3-8]. Then, single- or dual-axis solar trackers [9-18], the optimized solar cell configuration and geometry, new materials and technologies for optoelectronic applications, etc. [19-22] can be used for improving the efficiency of PV conversion. Although solar trackers can gain more energy, some problems appear in their installation such as high energy consumption, cost, the issue of (un)reliability and maintenance. It is not recommended to use a solar tracker for small panels because of high energy loss in the driving systems. It is shown that a tracking device increases energy while consuming very low amount of power (2 to 3%).

The strategic choice of Algeria, a country located in the Northern Africa on the Mediterranean coast which ranges in latitude from 18.96 south to 37.09 north and in longitude from 8.69 west to 11.95 east, has a significant solar potential for renewable energy in the world, recovered from sunlight reaching 3900 h, particularly in the Sahara desert. An Algerian map of solar radiation demonstrates solar energy potentials of this specific zone which provides useful information for optimum plant selection of solar energy system [23]. This map can be used as a database for future investments in solar energy, showing that the highest intensity is detected to be around the area of Djanet (southern Algerian desert) and the less intense area is identified to be around Ksar Chellala (Tiaret High Planes).

In 2007, the first hybrid plant in the world was constructed in Hassi R'Mel in the southern Algerian desert. It is an ISCC (Integrated Solar Combined Cycle) composed of a conventional combined cycle and a solar field with a nominal thermal power of 150 MW. The goal of this project was to integrate the solar thermal technology into a conventional power plant which integrates a solar field of CCP (parabolic through collector) covering a reflective area of 180,000 m^2. This combined use reduces the cost and facilitates the deployment of renewable energies in newly industrializing countries. The power plant will be constructed in Boughezoul, on the northern edge of the Sahara desert (Aures), and will serve primarily as a pilot and research facility. It will be able to operate using just solar energy or as hybrid power plant fuelled by a combination of solar power and gas.

Algeria is engaged in a new age of sustainable energy use [24]. The program consists of installing up to 22 GW of power-generation capacity from renewable sources between 2011 and 2030, of which 12 GW will be intended to meet the domestic electricity demand and 10 GW destined for export. This last option depends on the availability of a demand that is ensured in the long term by reliable partners as well as attractive external funding. It is expected that about 40% of electricity for domestic consumption be produced from renewable energy sources by 2030. This document was produced by the Ministry of Energy and Mines, which was designed and printed by SATINFO, Sonelgaz Group Company.

In this context, this paper involves the design and control of the prototype of a dual-axis solar tracking system for solar PV panel to improve energy efficiency. Tracking system for solar PV panel improves the extraction of maximum solar energy. The system is composed of two basic parts: the mechanical assembly and electrical parts. The electric part is composed of four identical LDRs as the input, the ATMEGA microcontroller as the controller, and two servomotors as the output.

2. Solar tracking panels

Considering the geographic situation in Africa, Algeria enjoys one of the most important sunny capacities in the world with 2200 KWh/m^2/annum. The insolation in most areas of the annual national territories reaches 2000 hours and may reach 3900 hours in the Sahara. Daily received energy within a horizontal area of 1 m^2 is nearly 5 kWh in the major zones, 1700 kWh/m^2/annum on the northern side, and 2263 kWh/m^2/annum on the southern side of the country [24-27]. Sunny capacity exceeds 5000 TWh. Table 1 shows the solar potential in three principal zones (coast zone, high planes, Sahara) of the Algerian territory.

Solar trackers represented in Figure 1 are a field of PV panels mounted on a moving surface following the

Table 1. Solar potential in Algeria.

Zone	Coast zone	High planes zone	Sahara
Surface area (%)	4	10	86
Sunny mean period (hours/annum)	2650	3000	3500
Mean energy received (kWh/m^2/annum)	1700	1900	2650

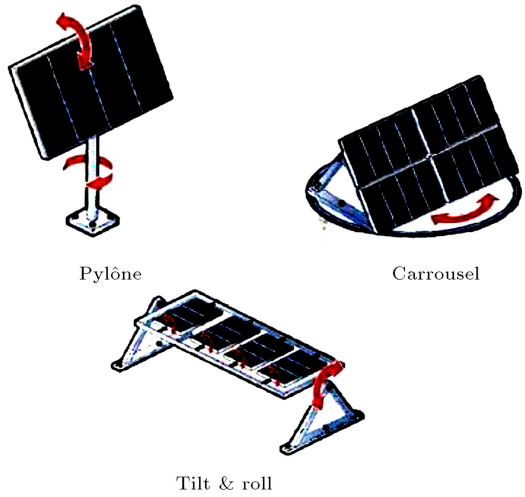

Figure 1. Classes of dual-axis solar trackers.

trajectory of the sun using dual-axis trackers. Using a single axis, the panels can be installed in an inclined plan with a fixed angle on a vertical pylon which will orient the PV field in the direction of the sun along the sunny day. The single-axis panel can be in the same plan of the inclined panels which will be tipping from east to west in the direction of the sun. A dual-axis solar tracker is mechanically more complex leaving the plan of the PV panels always in the perpendicular direction to the sun for any position in the sky.

The basic specifications which differentiate the trackers from stationary ones are the electrical production gain, mono or multi-axial orientation, robustness (against wind), reliability, and cost.

By using a dual-axis solar tracker, the PV modules produce up to 40% of energy per annum with differing significant production rates ($>$ 5 times) in higher consuming electrical energy hours at a cost of mechanical complexity and maintenance need [5].

3. Moving PV panels interest

Two basic widely used solar PV panels are the single- and dual-axis trackers. A single-axis tracker can have either a horizontal or a vertical axis. The dual-axis solar PV panel tracker is characterized by the capability to move in both horizontal and vertical directions. The vertical and horizontal motions of the panel are obtained by taking altitude and azimuth angles as references, making them able to track the sun's apparent motion anywhere in the world throughout the day in any seasons. Furthermore, during seasonal changes, latitudinal sun offset must be compensated.

During the day, the sun is moving continuously, contrary to the fixed position of PV generator that loses an enormous quantity of energy. To optimize the efficiency, the panels will be installed in the Algerian south area (Sahara). The energy collected by PV

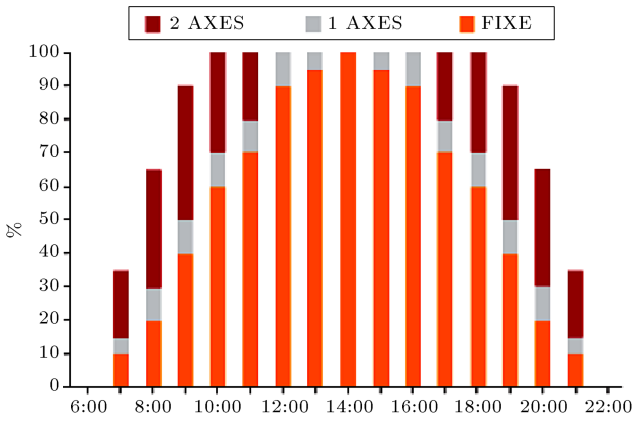

Figure 2. Efficiency comparisons of fixed support design and tracker panels.

panels is maximal only at midday, as seen in Figure 2. For this reason, if the PV panels are continuously oriented towards the sun, the maximal power will be provided for a long period of the day.

During a sunny day, a well-oriented system (of one kWp) provides 5.5 kWh of energy. The same tracker system, in the same sunny conditions, provides 11 kWh. Figure 2 illustrates the comparison results of their productions [5].

4. Methodology and technique of PV panels

This project involves designing a dual-axis tracker solar panel prototype, controlled by geared dc servomotors, and analysing its working and performance. It is composed of three main parts: Four LDRs forming the inputs, the Arduino Uno as the ATMEGA328P microcontroller, and two servomotors as the outputs where the block diagram is represented in Figure 3. Analog signals from the cadmium sulfide LDRs are captured by the ATMEGA328P, converted to digital signals by Analog/Digital converters, adjusted by two potentiometers (R_{TOL}, R_{VIT}), and sent to two PWM controlled servomotors to move panel towards the sun rays.

Figure 4 shows the LM 7805 positive voltage regulator providing +5 V required by the microcontroller and most of components of our realization.

The system is designed in two basic parts: the mechanical and electrical parts.

4.1. Different components of the electric design

This section concerns the components of the solar tracker to orient the panel towards solar rays. The components of the hardware design are four LDRs, the Arduino Uno microcontroller, and two servomotors.

4.1.1. Photoresistor

Light-Dependant Resistor (LDR) or Cds photocell, as shown in Figure 5(a), is composed of a high resistivity

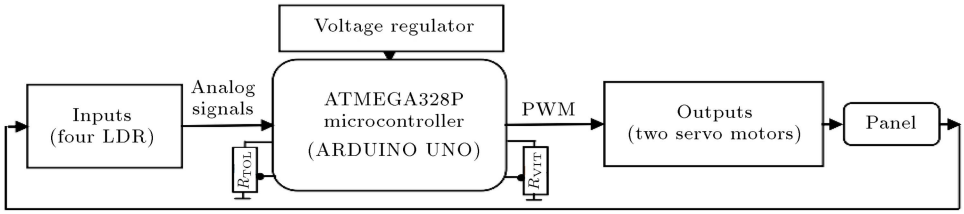

Figure 3. Block diagram of the overall system.

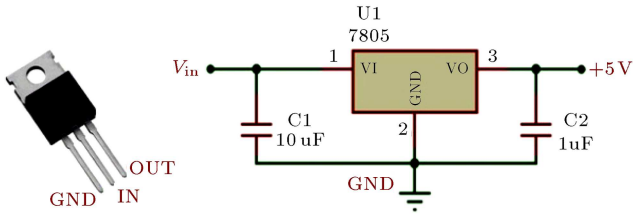

Figure 4. Voltage regulator.

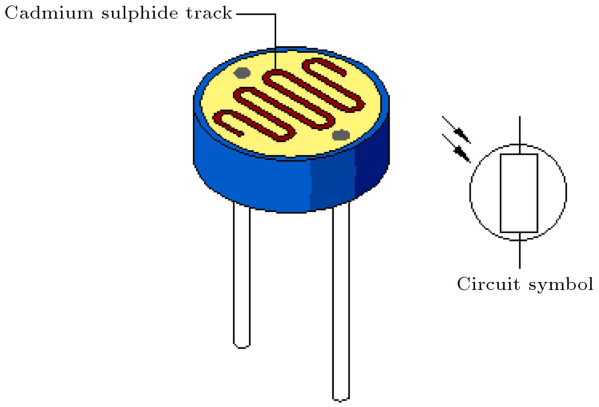

Figure 5(a). Cds LDR.

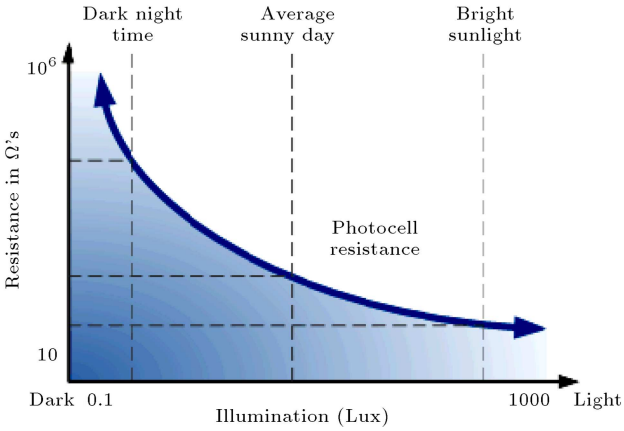

Figure 5(b). LDR characteristics.

semiconductor and is a component whose resistor value decreases exponentially when the sunlight intensity (illuminated as in lux) increases, as shown in Figure 5(b). This intensity of light sensed by the LDR is used as an analog input voltage for the ATMEGA microcontroller.

For our application, four identical LDRs are used in a sight glass disposed on the panel surface and

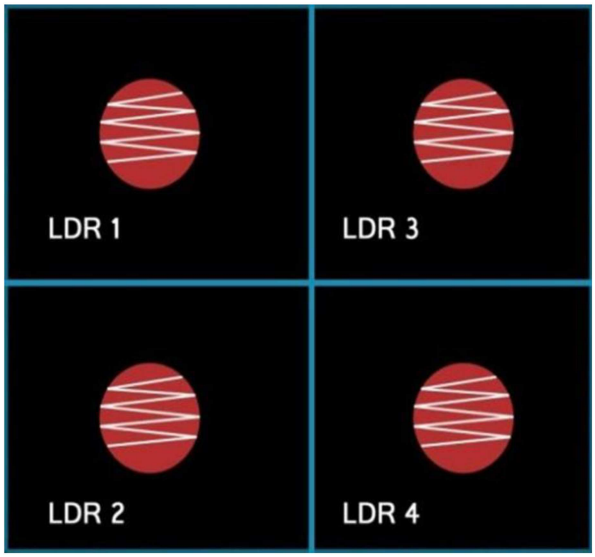

Figure 5(c). Sighting glasses composed of four LDR.

optically isolated by an opaque plate, as shown in Figure 5(c); thus, their illumination marks can be similar only if the sight glass is pointed toward the sun.

This sight glass is fixed on a PV panel and placed on the same plan, forming a sensor designed to detect the sun position. A signal error is generated if the system is non- pointed. It is the signal which will be used by the microcontroller to deliver the adequate control to dc servomotors. To process this signal, a voltage divider has been used for each LDR.

The output voltage V_{out} is proportional to the light intensity. V_{out} will increase when the maximum light is captured by the LDR, and V_{out} is weak when the LDR is in the shadow, expressed by:

$$V_{\text{out}} = \frac{V_{\text{in}}.R}{(R + R_{\text{LDR}})}. \tag{1}$$

4.1.2. Servomotors

The objective of servomotors is to provide an exact movement as a response to an external control. It is an actuator which mixes electronics, mechanics, and automatics. Servomotors' high torque servo with very large power range is available in a wide variety of frame sizes from small to large; it is capable of running huge machines, has an excellent power capacity to weight size ratio given their best efficiency (80-90%), and will do fine with low speed applications given low friction

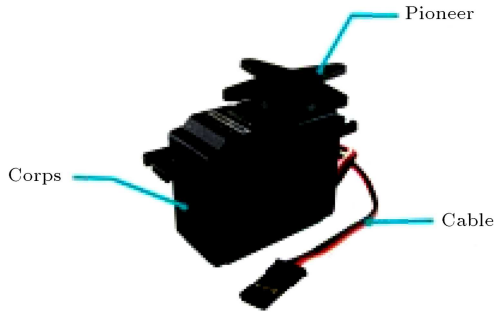

Figure 6. Servomotor blocks.

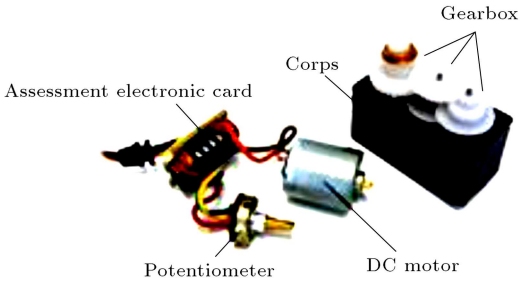

Figure 7. Different parts of the servomotor.

and the correct gear ratio leading to a very low heat production, vibration, and very little noise.

The servomotor in Figure 6 is an assembly of three basic blocks: a body comprising all the mechanics and electronics, a cable to lead power and the control (reference signal), and a pioneer attached to the servomotor's axis. Herein, the pioneer is attached to the mechanical parts to move (arm, wheel, etc.).

This servomotor type requires regulated supply voltage of 5 V. This consists of three wires: signal, positive, and ground wires.

It also comprises several internal parts that include the motor and gearbox, position sensor, an error amplifier, motor driver, and a circuit to decode the requested position. The servomotor only rotates by the maximum of 180 degrees.

4.1.3. The internal servomotor structure

The servomotor used in this project is an assembly of four parts: an electrical dc motor, a gearbox, a position-sensing device which is usually a potentiometer, and an electronic card to control and assess the motor.

The servomotor body is composed of an electronic card receiving the reference signal to do the assessment. This card controls an electrical dc motor that will drive the pioneer through the speed-reducing gear, as illustrated in Figure 7.

The gearbox has two functions:

- Reducing the speed to provide an accurate tracking of relative position of the servomotor and avoiding any system damage when movement is driven by its speed if it is very high;

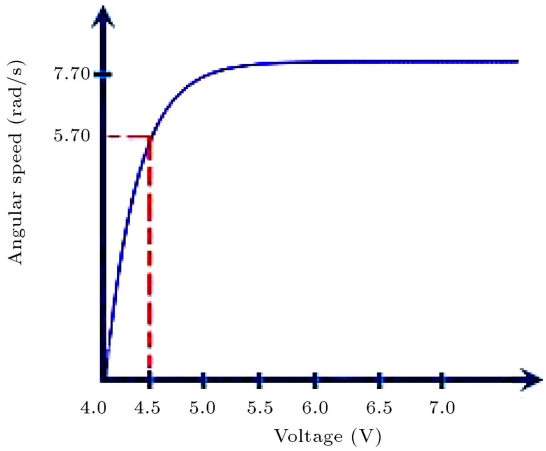

Figure 8(a). Motor angular speed versus supplying voltage.

- Increasing the torque by its mechanical movement of rotation. At an instant t, if we decrease speed Ω leaving the same mechanical power P_{mec}, this will increase torque T.

Figure 8 shows a dc servomotor response of rotating speed via supplying voltage, $\Omega = f(U)$, electromagnetic torque via the armature current, $T = f(I_a)$, and torque via angular speed, $T = f(\Omega)$.

Speed and current are related to supplying voltage and electromagnetic torque, respectively. Hence, for a given fixed speed, if our system increases the mechanical power to move a heavier load (solar panel weight), this will increase current (considering that U and Ω remain constant and electrical power, $P_{el} = U.I$, must be equal to mechanical power, $P_{mec} = T.\Omega$, all internal losses are neglected). Since the consumed energy by the system is generated by the panel itself, to improve efficiency, power consumption of the solar tracker is reduced since the servomotors supply the amount of torque just sufficient enough to move it (its mass is about 250 g).

Figure 8(a) shows angular speed, Ω, of the servomotor changed with the output voltage, U, of the drive unit. The speed, Ω, starts obviously at zero (servomotor at rest) to reach its maximal value by 7.8 rad/s. It is observed that Ω increases in a linear manner with voltage U to stabilize at an approximate specific value for 5 V.

Figure 8(b) shows the evolution of torque, T, via current, I. The drive unit controls the output torque linearly, starting at $T_L = 16.3$ kg cm, to increase with current.

Figure 8(c) shows the evolution of T via Ω. it is noticed that the servomotor keep its torque value even when its speed increases; however, when the motor reaches its nominal speed of 7.7 rad/s, servomotors supply the amount of torque (10 kg.cm) just sufficient enough to move it.

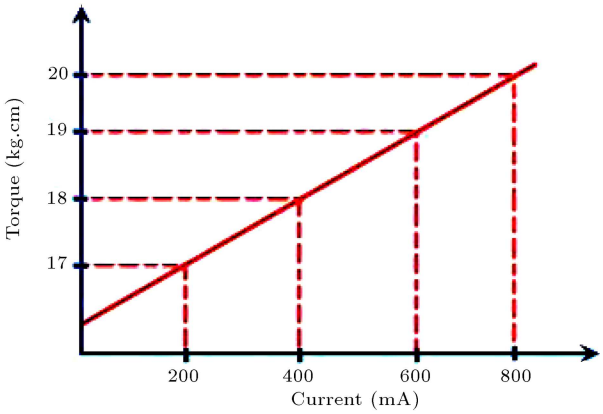

Figure 8(b). Torque versus armature current.

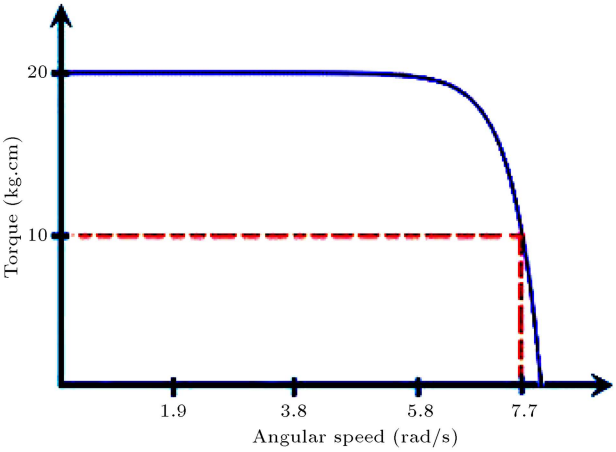

Figure 8(c). Torque versus angular speed.

4.2. Servomotor's performance and working

PWM is used to control the motors. A PWM analog signal will go through an electronic circuit and convert the analog signal into a digital signal. PWM in servos is used to control the direction and position of the motor. Two servomotors are used in this project for horizontal and vertical axes.

Servomotors are controlled using an electrical cable composed of three wires to supply the motor (positive and ground), and the third one is used to transmit a PWM analog signal to control the motor's positions. This means that it is the period of impulsions that determines the absolute angle of the output axis and, then, the position of the control shaft of the servomotor. The signal is periodically repeated, in general, every 20 milliseconds, as shown in Figure 9. This permits electronics to control and continuously correct the output axis angular position. This one is measured by the potentiometer. When the servomotor rotates, the axis of the servomotor changes the position that will modify the potentiometer resistance. The role of the electronic circuit is to control the motor so that output axis position can conform to the received reference signal.

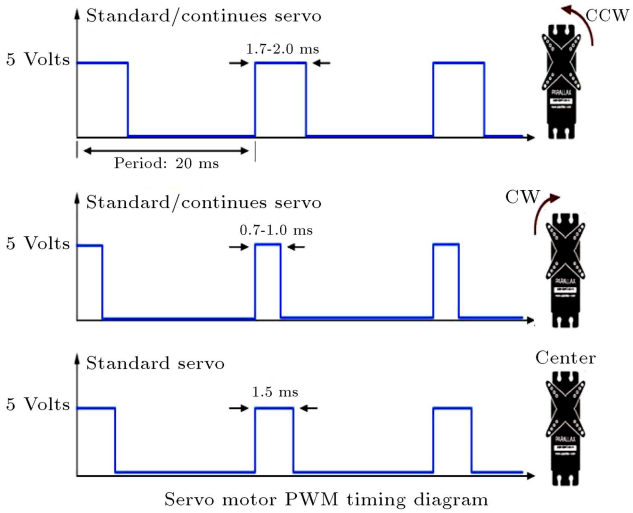

Figure 9. Position of the pioneer relative to the PWM signal.

5. Microcontroller and programming

Our active sun tracker is controlled by PC program using an Arduino Uno. This section presents the specifications of the microcontroller and the developed programming to conduct the exact system working.

5.1. The microcontroller

5.1.1. Advantages of the microcontroller

The use of microcontrollers for programming circuits comes with various strong and real advantages. In fact, we have found the spectacular evolution of IC (Integrated Circuit) design in recent years.

It encompasses various components decreasing the cumbersomeness of materials and IC, simplifying the tracing of printed circuits to data/address bus, increasing system reliability, and reducing cost.

5.1.2. Microcontroller role in a solar tracker system

The microcontroller converts the analog signal captured from LDR to the digital signal which will be compared to a tolerance input signal, to be transmitted to the servomotors in order to move the PV panels where it can receive the maximum amount of sunlight.

5.1.3. Microcontroller choice

Many designers propose microcontrollers (Microchip, Atmel, Texas-Instrument, Free Scale, NXP, Cypress, etc.). Each one proposes various families of microcontrollers (PIC and dpPIC from Microchip; AVR, AVR32 and ARM from Atmel, etc.). Each family contains tens of models, which are basically different with respect to their memory sizes and the I/O pins number.

The choice of the microcontroller is done on the basis of its application: its preference to fix a family. Even though the PIC microcontroller of Microchip has contributed much to popularise the architecture Reduced Instruction Set Computer (RISC) and a great

deal of information in the world of microcontrollers and in the related literature has been devoted to informatics architectures, they are not the only circuits in the market. The microcontrollers of AVR family from Atmel, to which this paper is dedicated, use this architecture and, hence, benefit from various advantages.

The AVR family has many advantages: inexpensive, low-energy consumption, and a good support multi-platform. They are successful, given the following specifications:

(a) Easy C++ programmation for most basic functions;

(b) Low cost and large availability;

(c) Low-energy consumption.

5.1.4. ATMEGA microcontroller

The microcontrollers of the family ATMEGA, in CMOS technology, are models of 8-bit AVR based on architecture RISC. When instructions are executed in a simple clock cycle, the ATMEGA realizes operations reaching 1 MIPS by MHZ allowing for simple systems design and low-energy consumption.

5.1.5. Structure of an ATMEGA microcontroller

The ATMEGA328P microcontroller is characterized by the following particularities:

- A Flash Memory of 32 KB for program storage;
- A SRAM Memory of 2 KB for variables storage;
- An EEPROM Memory of 1 KB for permanent robot parameters storage;
- Technology RISC (one instruction per clock cycle) presenting a power of 20 Million Instructions Per Second (MIPS) for a clock frequency of 20 MHz;
- An UART (Universal Asynchronous Receiver/ Transmitter) compatible RS232 for the communication with the PC;
- I2C bus for the communication with the components I2C;
- An analog/digital converter ADC of 6 channels of 10 bits;
- Supplying voltage of 2.7 V to 5.5 V.

5.1.6. Synopsis

Figure 10 shows the synopsis of the internal hardware architecture of the ATMEGA328P microcontroller.

5.1.7. Pins description

It is an IC of 28 dual in-line pins shown in Figure 11 in which 14 are the digital input/output, of which 6 are PWM outputs, 6 are analog inputs, a 16 MHz quartz crystal oscillator, an ICSP (In Circuit Serial Programming) header, an USB connection, a power jack, and a reset button. Each pin function is described below:

- VCC: supplying voltage (+3 V to +5 V);
- GND: ground;
- Port B (PB7... PB0): it is a bidirectional I/O port of 8 bits with internal pull-up resistors chosen for each bit;
- PB6/XTAL1: External oscillator amplifier input or free for internal clock;
- PB7/XTAL2: Output of the oscillator amplifier;
- Port C (PC5... PC0): It is a bidirectional I/O port of 7 bits with internal pull-up resistors selected for each bit;
- PC6/RESET: Released by falling front maintained for more than 50 ns producing the reset of microcontroller, even if the clock is at rest;
- Port D (PD7... PD0): The port D is a bidirectional I/O port of 8 bits with internal pull-up resistors chosen for each bit. It is used as a USART and inputs for external interruptions;
- AVcc: It is supplying voltage to the pin for the A/D converter which must be connected to Vcc via low pass filter to avoid parasites;
- AREF: It is the analog reference input for the A/D converter with a voltage of 2 V to AVcc with low-pass filter.

5.1.8. Oscillator

The external quartz crystal oscillator is connected to XTAL1 and XTAL2, as shown in Figure 12, to run the microcontroller. Crystal type Quartz frequency is from 4 to 16 MHZ or ceramic resonator.

Using the external quartz oscillator, a capacitive damper of about 12 to 22 pF must be connected, as shown in Figure 12.

5.1.9. A/D Converter (ADC)

The analog to digital converter integrated into the ATMEGA comes with very interesting specifications such as a 10-bit resolution and 6 simultaneous inputs. This ADC converts the analog voltage to digital signal coded on a 10-bit resolution described by resolution Eq. (2):

$$\text{Resolution} = \left(\frac{V_{\text{in}}}{V_{A.\text{ref}}} \times 1024\right) - 1. \tag{2}$$

5.2. Design of the solar tracker control circuit

A dual-axis tracker based on four identical LDRs was constructed and tested to set the optimal values of potentiometers R_{VIT} and R_{TOL}, shown in both Figure 3 and Figure 13. The R_{TOL} tolerance was calculated in terms of the angle between the upside couple of (LDR1, LDR3) and downside couple of (LDR2, LDR4) sensors. After some initial and trial error testing, the optimal angle between these photo-resistors was

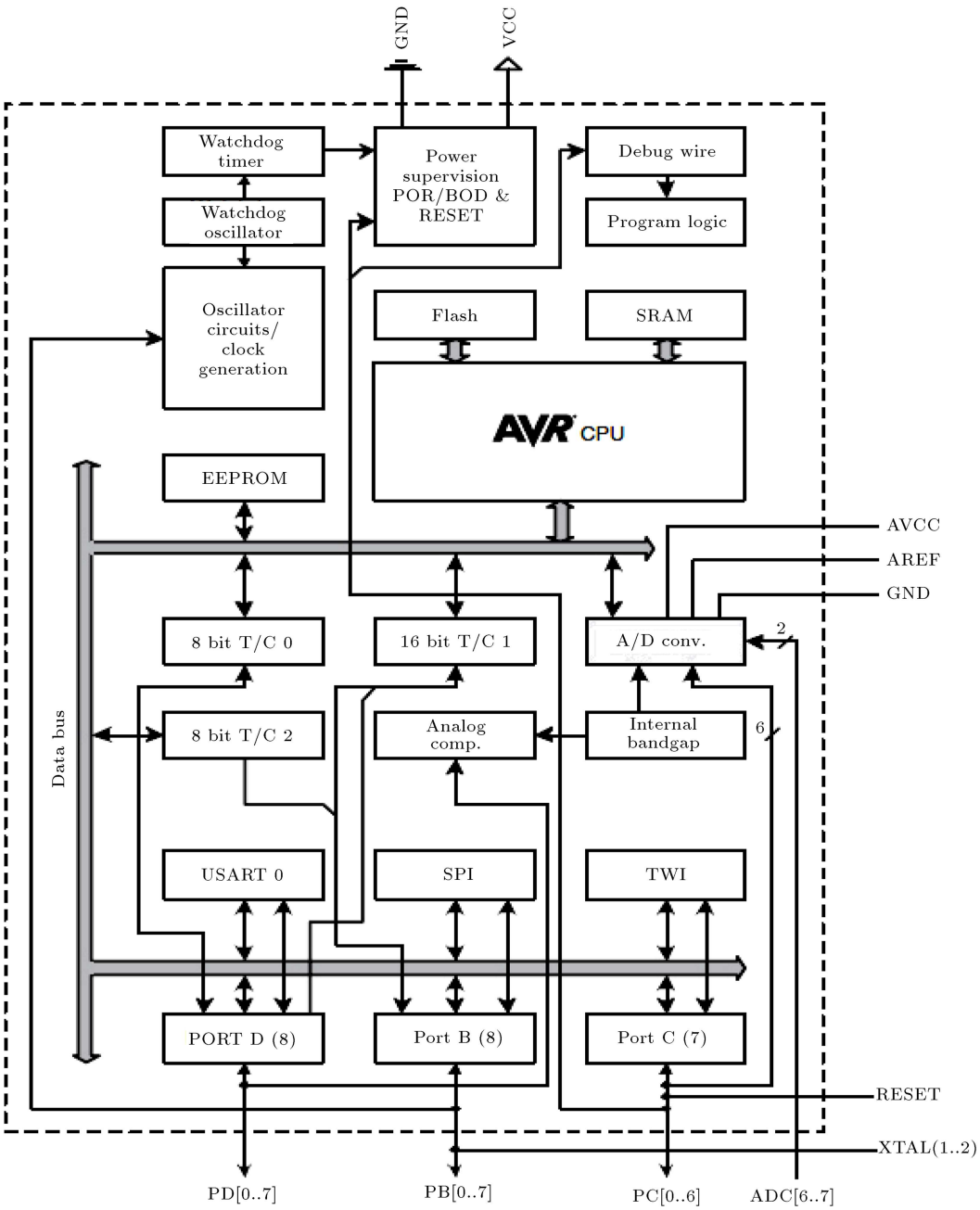

Figure 10. Synopsis of the ATMEGA328P.

evaluated experimentally to set the tolerance voltage value TOL. Precise results were found because the system was working in a close-loop system, which is the conventional control method of sun tracking systems by the photo sensors. The photo sensors are used to discriminate the sun's position and, then, send the proper analog electrical signals, converted to the digital signal, proportional to controller error, which actuates the motors to track the sun [17,28]. A circuit scheme of the designed system for horizontal and vertical axes is shown in Figure 13. When the sun moves to the east or to the west, either the couple (LDR3, LDR4) or (LDR1, LDR2) will receive more light, transforming the collected solar light intensity to electrical voltages $V_{\mathrm{LDR3,4}}$ or $V_{\mathrm{LDR1,2}}$ using the voltage dividers (Eq. (1)). Then, they are sent to ADC ports (P_{c0}, P_{c1}) for the altitude angle or ports (P_{c2}, P_{c3}) and for the azimuth angle tracking to the microcontroller to make a comparison with the tolerance input signal TOL sent to ADC port (P_{c5}) to control servomotors. These ports perform the orientation of the PV panel towards the sun. Rotation directions for the azimuth and altitude angles tracking the respective horizontal (H) and vertical (V) motors are controlled by

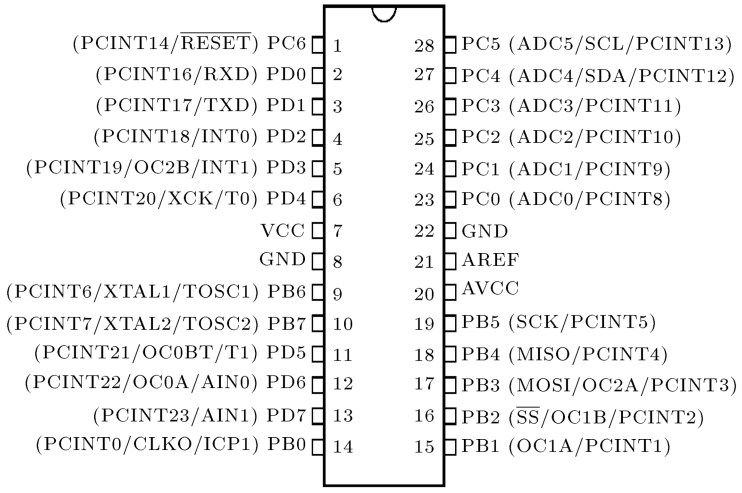

Figure 11. ATMEGA328 typical pins.

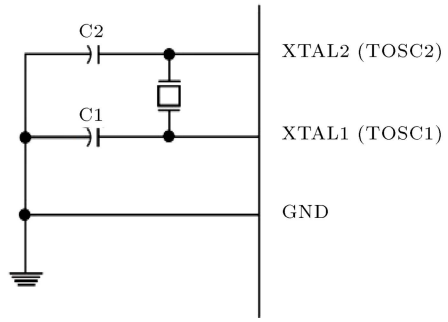

Figure 12. Oscillator circuit.

using two differential amplifiers (op-amp-H, op-amp-V). Couples ($V_{\mathrm{LDR3,4}}$, $V_{\mathrm{LDR1,2}}$) and ($V_{\mathrm{LDR1,3}}$, $V_{\mathrm{LDR2,4}}$) voltages are sent to the microcontroller for average computation and comparison with TOL. According to the average differences between the voltages from LDR couples, $d_{\mathrm{Vert}} = |\mathrm{mean}(V_{\mathrm{LDR1,3}} - V_{\mathrm{LDR2,4}})|$ or $d_{\mathrm{Horiz}} = |\mathrm{mean}(V_{\mathrm{LDR1,2}} - V_{\mathrm{LDR3,4}})|$ are bigger or smaller than the fixed value TOL; the proper logic signals are sent to the errors op-amps to drive the dc motors. The width of a PWM control signal shown in Figure 9, generated by using AVR timers, determines the absolute angle of the output axis and, then, the position of the control shaft of servomotors. When the motors rotate, H and V axes change the positions that will accordingly modify the potentiometers' resistance (position sensors of the assessed electronic card in Figure 7) mounted on the shafts and provide H and V with feedback voltages. They will be compared to PWM control signals to determine the positions of the dc motors. Finally, H-motor and V-motor are turned in such directions as clockwise (cw) or counter-clockwise (ccw) that the absolute values of d_{Horiz} and d_{Vert} become less than the TOL value, and the motors then stop. When the light sensors have the same amount of resistance values (i.e., for the same rate of light), the error amplifiers give the same output (0 V) (i.e., the sight glass in Figure 5(c) is pointed towards the sun), and since the potential difference at the motor terminals is zero, the panel does not rotate.

The logic ISIS Proteus is used to simulate our montage in Figure 13. The assemblage of different parts of the system is presented on the global electric scheme of the installation, represented as follows.

The optimal value of potentiometer R_{VIT} is set based on the weight of the PV panel. For our system, R_{VIT} is fixed to 2.5 kΩ.

If a very small value of the tolerance is chosen, e.g., TOL=0.0001 V, our panel surely oscillates. Potentiometer R_{TOL} will be taken which has a tolerance of 0.5 V for a proper working of our system.

5.3. Developing environment

The compiler gcc-avr has been chosen which is compatible with the most popular platforms (Windows, Linux, and Mac).

To transmit the software PC program to the Atmega328p microcontroller, conversion USB series module must be used; it is the FTDI Basic Breakout in the same card comporting a microcontroller noted Arduino Uno.

Arduino Uno developing environment is a Java multi-Platform application, used as a code editor and a compiler, to transmit codes to asynchronous serial liaison using C++ programming language.

The Atmega328P pin mapping with Arduino Uno board is shown in Figure 14 for its programming using C++ language illustrated in Appendix A.1.

6. Various steps of the mechanical design

This section presents the design of the mechanical parts adopted for the solar tracking mode working on the basis of horizontal and vertical directions of varying angles from 0° to 180° and from 0° to 90°, respectively.

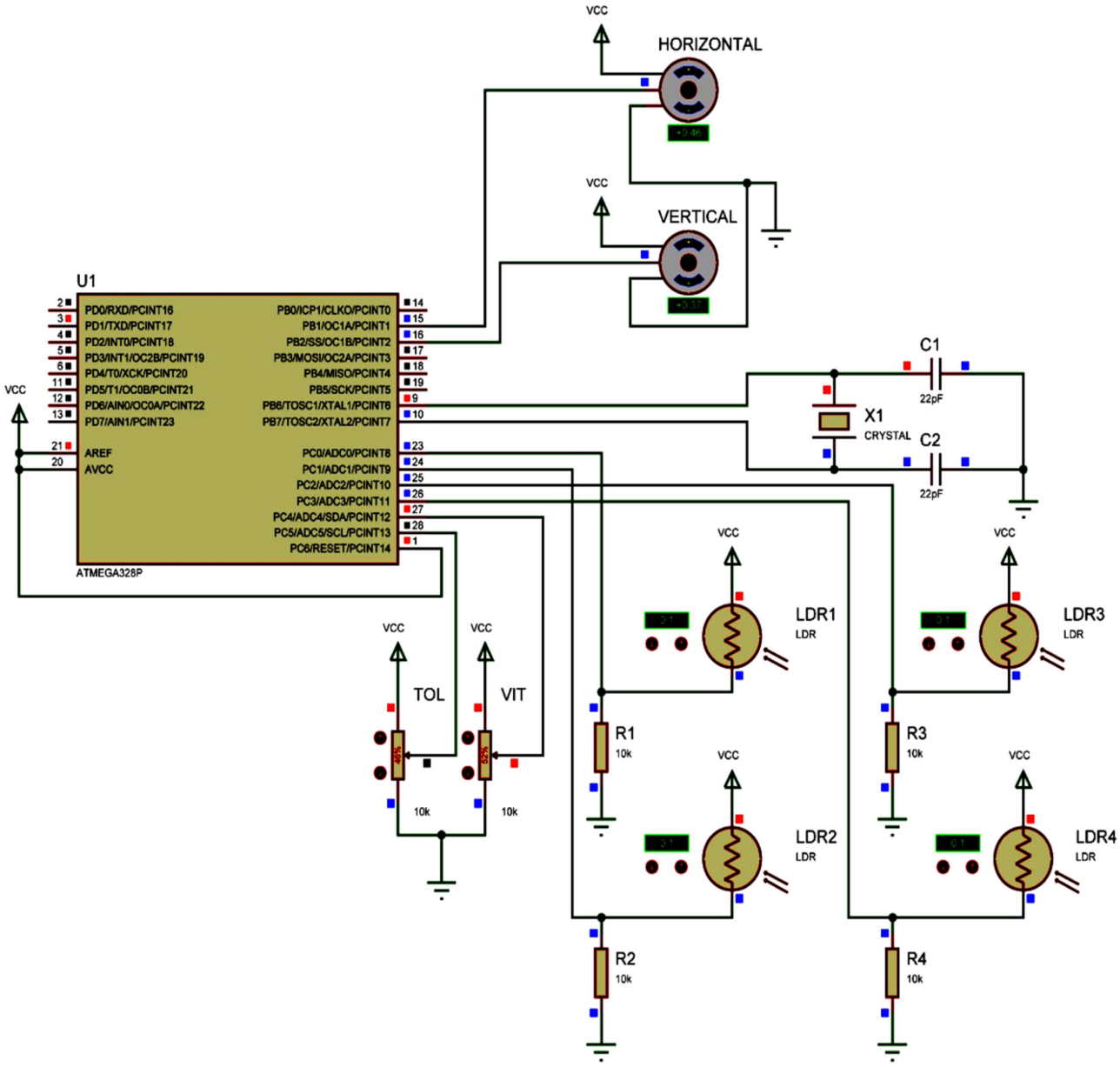

Figure 13. Solar tracker control circuit.

The mechanical design consists of rotary joints and two dc servomotors.

6.1. Photovoltaic panel prototype

Figure 15 shows our design as a prototype composed of a wooden plate. Its size is 460 × 285 mm and its mass is about 250 g. This woody plate will be fixed by seven vices in seven points on the vertical axis: three in front and four behind.

6.2. The sight glass

Figure 16 shows the sight glass which is fixed to the photovoltaic panel prototype and placed on the same plan. It is composed of four LDRs disposed in cross and optically isolated from each other; consequently, the light intensities will not be identical only if the sight glass is pointed towards the sun.

6.3. Vertical axis

The vertical axis is realized in wood size of 390 mm, the same for each side. Dual ball bearing facilitates their rotation. Figure 17 shows how we have fixed the servomotor HS-645MG standard deluxe on the one side.

6.4. Horizontal axis

It is realized that ball bearing will be in the middle of the axis as shown in Figure 18 in order to be able to drive the sole.

6.5. The basis

The axis is realized in wood size of 390 × 390 mm, as

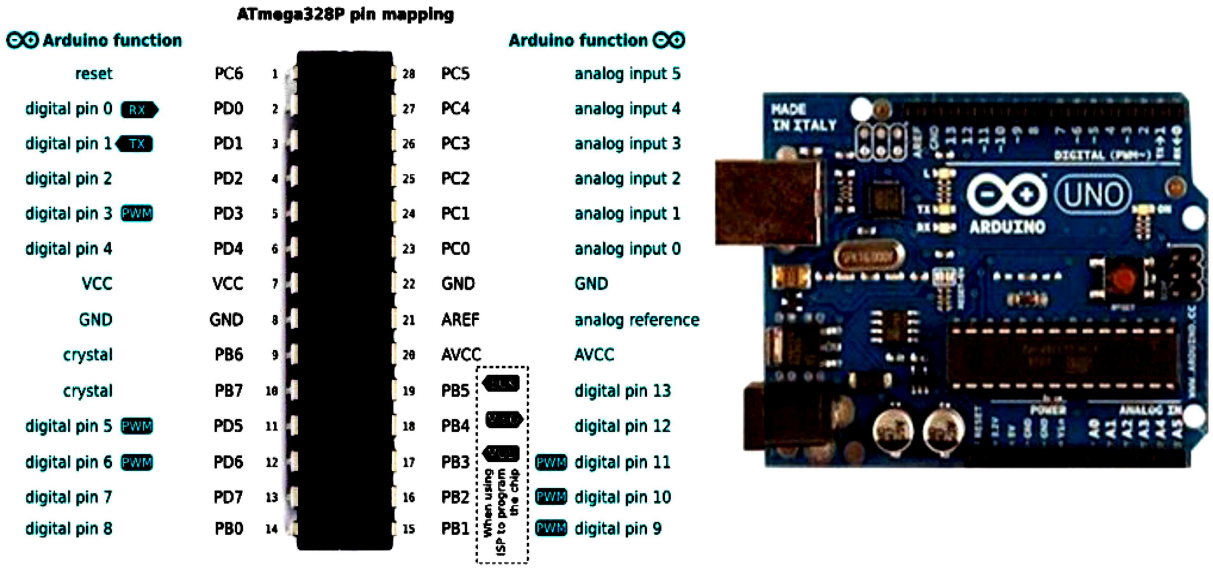

Figure 14. Atmega328P pin mapping with Arduino Uno board.

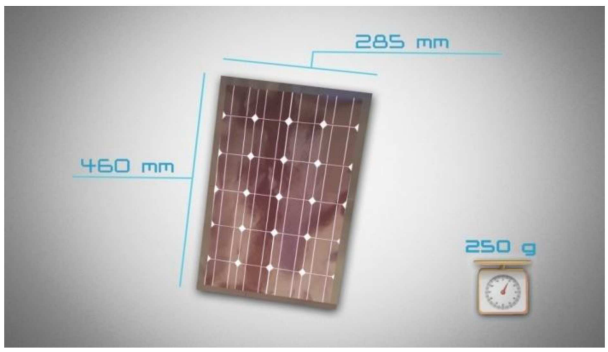

Figure 15. Photovoltaic panel prototype.

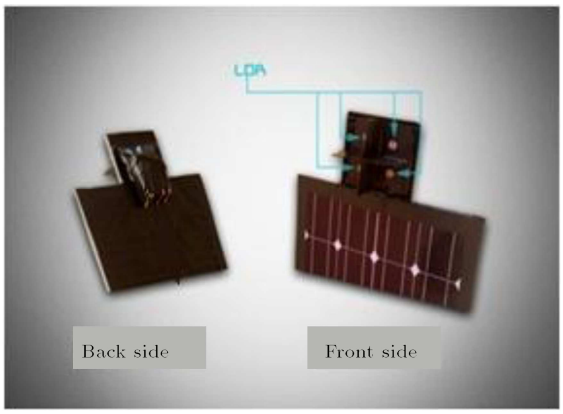

Figure 16. Sight glass of the tracker.

shown in Figure 19. Its role is to insure the size and the stability of the installation.

To orient the panel towards the solar rays, we must, first of all, make the choice of the motors.

The size of the tracker panel prototype is imposed by the torques of servomotors. These constraints have

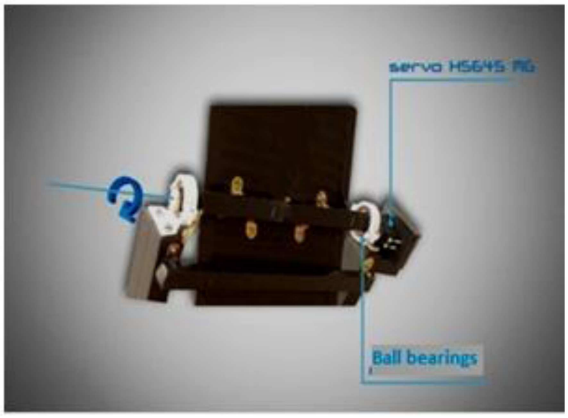

Figure 17. Vertical axis of the tracker.

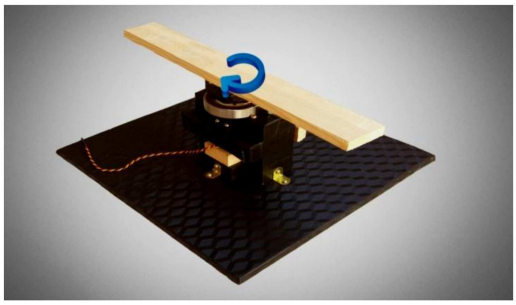

Figure 18. Horizontal axis of the tracker.

conducted the design of an experimental tracker where the quotations are mentioned in Figure 20 (340 mm × 275 mm).

7. Management of system flowchart

The global program intended to a programmable circuit is based on a precise idea to satisfy the constructor

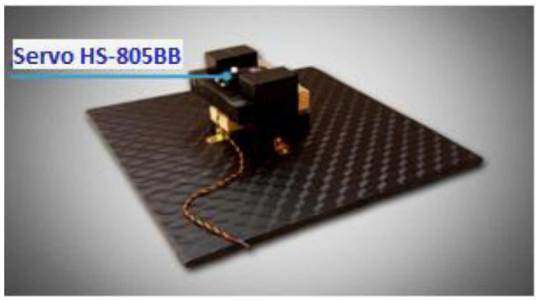

Figure 19. Tracker basis.

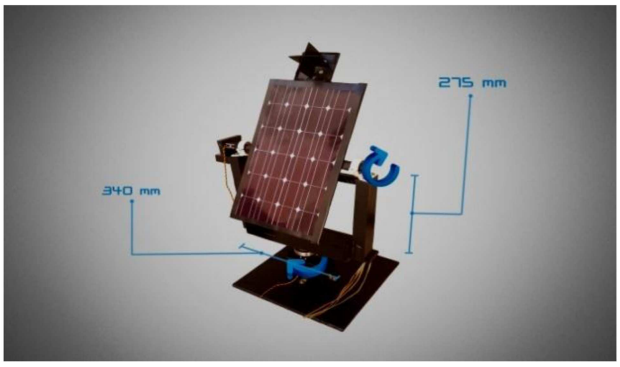

Figure 20. Prototype of the tracker panel.

catalogue and industrial context. This one is generally translated through a flowchart defining the various steps of the program.

Basic software design

The basic software flowchart of the solar tracker system is illustrated in Appendix B.

8. Conclusion

The described program satisfied the control conditions for the good working of the system; hence, results are encouraging. In fact, the program repartition allows to distinguish various realized operations. Instructions were derived from the program guidelines in the methodical repairing of the functions. It facilitated the modifications which could be made during these works. The proposed montage used a limited number of components which are easy to use and occupied a restricted space which could be integrated into a complete photovoltaic system. The total cost reached only 150 Euros, and the period of realization is about 40 days. It has an effective contribution to the environment and could be improved. Two degrees of freedom orientation were made able to track the sun position. In our case, the system was tested using the flash-light of a moving electrical lamp to shine it at the sensors; the tracker followed it around, which was successful in verifying its efficient and correct working. The microcontroller was used to control exact shaft position of dc servomotors which ensured the point-to-point intermittent stable movement. The microcontroller was designed to rotate the panel from 0 to 180 degrees. The presented dual-axis solar panel tracking system keeps the solar photovoltaic panel perpendicular to the sun throughout the year to improve the efficiency of the system.

As advancements made in photovoltaic trackers technology have decreased investment prices, this project could be extended to power supply fit for isolated villages or farms by mounting highly optimal, large and scheduled moving panels to provide a huge amount of solar energy. Scheduled tracking must use a computer program to change the angle of the panel based on date, time, and its physical location even under cloud coverage.

References

1. Finster, C. "University Santa Maria Heliostat" [El Heliostato de la Universidad Santa Maria], *Scientia*, **119**, pp. 5-20 (1962).
2. Saavedra, A.S. "Design of a sun tracking mechanism for automatic measurement of direct solar radiation" [Diseno de un servomecanismo seguidor solar para un instrumento registrador de la irradiación solar directa], Memoria, Technical University Federico Santa Maria, Valparaiso, Chile (1963).
3. Abdallah, S. and Nijmeh, S. "Two axes sun tracking system with PLC control", *Energy Conversion and Management*, **45**(11-12), pp. 1931-1939 (2004).
4. Roth, P., Georgiev, A., and Boudinov, H. "Cheap two-axis sun following device", *Energy Conversion and Management*, **46**(7-8), pp. 1179-1192 (2005).
5. Yazidi, A., Betin, F., Notton, G., and Capolino, G.A. "Low cost two-axis solar tracker with high precision positioning", *Proceedings of the International Symposium on Environment, Identities & Mediterranean Area ISEIM'2006*, Corte-Ajaccio, France, pp. 211-216 (July, 2006).
6. Rustemli, S., Dincadam, F., and Demirtas, M. "Performance comparison of the sun tracking system and fixed system in the application of heating and lighting", *Arabian J. Sci. Eng.*, **35**(2B), pp. 171-183 (2010).
7. Eke, R. and Senturk, A. "Performance comparison of a double-axis sun tracking versus fixed PV system", *Solar Energy*, **86**(9), pp. 2665-2672 (2012).
8. Lazaroiu, G.C., Longo, M., Roscia, M., and Pagano, M. "Comparative analysis of fixed and sun tracking low power PV systems considering energy consumption", *Energy Conversion and Management*, **92**, pp. 143-148 (2015).
9. Chang, T.P. "Output energy of a photovoltaic module mounted on a single axis tracking system", *Applied Energy*, **86**(10), pp. 2071-2078 (2009).
10. Sefa, I., Demirtas, M., and Çolak I. "Application of one-axis sun tracking system", *Energy Conversion and Management*, **50**(11), pp. 2709-2718 (2009).

11. Ponniran, A., Hashim, A., and Joret, A. "A design of low power single axis solar tracking system regardless of motor speed", *Internal Journal of Intergrated Engineering*, **3**(2), pp. 5-9 (2011).

12. Huang, B.J., Ding, W.L., and Huang, Y.C. "Long-term field test of solar power generation using one axis 3-position sun tracker", *Solar Energy*, **85**(9), pp. 1935-1944 (2011).

13. Seme, S., Stemberger, G., and Vorsic, J. "Maximum efficiency trajectories of a two axis sun tracking system determined considering system consumption", *IEEE Trans Power Electron*, **26**(4), pp. 1280-1290 (2011).

14. Koussa, M., Cheknane, A., Hadji, S., Haddadi, M., and Noureddine, S. "Measured and modelled improvement in solar energy yield from flat plate photovoltaic systems utilizing different tracking systems and under a range of environmental conditions", *Applied Energy*, **88**(5), pp. 1756-1771 (2011).

15. Saravanan, C., Panneerselvam Dr., M.A., and William Christopher, I. "A novel low cost automatic solar tracking system", *International Journal of Computer Applications*, **31**(9), pp. 0975-8887 (October, 2011).

16. Mousazadeh, H., Keyhani, A., Javadi, A., Mobli, H., Abrinia, K. and Sharifi, A. "A review of principle and sun-tracking methods for maximizing solar systems output", *Review Sustain Energy Ren*, **13**(8), pp. 1800-1818 (2009).

17. Yilmaz, S., Ozcalik, H.R., Dogmus, O., Dincer, F., Akgol, O., and Karaaslan, M. "Design of two axes sun tracking controller with analytically solar radiation calculation", *Renewable and Sustainable Energy Review*, **43**, pp. 997-1005 (2015).

18. Yao, Y., Hu, Y., Gao, S., Yang, G., and Du, J. "A multipurpose dual-axis solar tracker with two tracking strategies", *Renewable Energy*, **72**, pp. 88-98 (2014).

19. Nakano, Y. "Ultra-high efficiency photovoltaic cells for large scale solar power generation", *Ambio*, **41**(2), pp. 125-131 (2012).

20. Ghaedi, A., Abbaspour, A., Fotuhi-Friuzabad, M., and Parvania, M. "Incorporating large photovoltaic farms in power generation system adequacy assessment", *Scientia Iranica, Transactions on Electrical Engineering*, **21**(3), pp. 924-934 (2014).

21. Zerhouni, F.Z., Zerhouni, M.H., and Zegrar, M. "Modelling polycristallin photovoltaic cells using design of experiments", *Scientia Iranica, Transactions on Electrical Engineering*, **21**(6), pp. 2273-2279 (2014).

22. Dattaa, A., Bhattacharyab, G., Mukherjeec, D., and Sahad, H. "An efficient technique for controlling power flow in a single stage grid-connected photovoltaic system", *Scientia Iranica, Transactions on Electrical Engineering*, **21**(3), pp. 885-897 (2014).

23. Yaiche, M.R., Bouhanik, A., Bekkouche, S.M.A., Malek, A., and Benouaz, T. "Revised solar maps of Algeria based on sunshine duration", *Energy Conversion and Management*, **82**, pp. 114-123 (2014).

24. Stambouli, A.B. "Promotion of renewable energies in Algeria: Strategies and perspectives", *Renewable and Sustainable Energy Reviews*, **15**(2), pp. 1169-1181 (2011).

25. Adouane, M., Haddadi, M., Touafek, K., and Aitcheikh, S. "Monitoring and smart management for hybrid plants (photovoltaic-generator) in Ghardaia", *Journal of Renewable and Sustainable Energy*, **6**(2), 023112 (2014).

26. Yacef, R., Mellit, A., Belaid, S., and Sen, Z. "New combined models for estimating daily global solar radiation from measured air temperature in semi-arid climates: application in Ghardaia, Algeria", *Energy Conversion and Management*, **79**, pp. 606-615 (2014).

27. Behar, O., Khellaf, A., and Mohammedi, K. "Comparison of solar radiation models and their validation under Algerian climate - The case of direct irradiance", *Energy Conversion and Management*, **98**, pp. 236-251 (2015).

28. Bentaher, H., Kaich, H., Ayadi, N., Ben Hmouda, M., Maalej, A., and Lemmer, U. "A simple tracking system to monitor solar PV panels", *Energy Conversion and Management*, **78**, pp. 872-875 (2014).

Appendix A

C++ tracking control programm is shown in Figure A.1.

Appendix B

The basic software flowchart of the solar tracker system is shown in Figure B.1.

Explanation of the flowchart

We start with the configuration and initialization of I/O ports.

It is the nomination of the type of configuration of inputs or outputs ports indicating the used pins.

LDRlt = 0; $\longrightarrow$ LDR top left,

LDRrt = 1; $\longrightarrow$ LDR top right,

LDRld = 2; $\longrightarrow$ LDR down left,

LDRrd = 3; $\longrightarrow$ LDR down right.

Stand horizontal and vertical servomotors to the following angles values:

servoh = 90 degrees; $\longrightarrow$ stand horizontal servo,

servov = 90 degrees; $\longrightarrow$ stand vertical servo.

After delay times and system start up, compute mean values per sensors pair for the four sides shown in Figure (5c):

- *Read the analog inputs:* Acquire and convert the analog signal to digital values captured by the sensors;

```
// C++ program compilation
#include <Servo.h>      // include Servo library. Include the class of Servo.h, allow for easily
                           manipulating the complete management of servo motor
Servo horizontal;       // horizontal servo. Create "initialize the object servo"
int servoh = 90;        // stand horizontal servo

Servo vertical;         // vertical servo
int servov = 90;        // stand vertical servo

// LDR pin connections
// name = analogpin;

int ldrlt = 0;    // LDR top left
int ldrrt = 1;    // LDR top rigt
int ldrld = 2;    // LDR down left
int ldrrd = 3;    // LDR down rigt

void setup()
{
  Serial.begin (9600);
// servo connections
// name.attacht(pin);
  horizontal.attach(9);
  vertical.attach(10);
}
void loop()
{
  int lt = analogRead(ldrlt);     // top left
  int rt = analogRead(ldrrt);     // top right
  int ld = analogRead(ldrld);     // down left
  int rd = analogRead(ldrrd);     // down right


  int dtime = analogRead(4)/20; // Read potentiometers
  int tol = analogRead(5)/4;

  int avt = (lt+rt)/2;      // Average value top
  int avd = (ld+rd)/2;      // Average value down
  int avl = (lt+ld)/2;      // Average value left
  int avr = (rt+rd)/2;      // Average value right
  int dvert = avt-avd;      // Check the difference of up and down
  int dhoriz = avl-avr;     // Check the difference of left and right

  if (-1*tol > dvert||dvert > tol) // Check if the difference is in the tolerance else change vertical angle
  {

if (avt > avd)
{
 servov = ++servov;
 if (servov > 180)
 {
 servov = 180;
 }
}
else if (avt < avd)
{
 servov= –servov;
 if (servov < 0)
{
 servov = 0;
```

Figure A.1. Tracking control C++ program.

```
  }
  }
  vertical.write(servov);
  }

  if (-1*tol >dhoriz —dhoriz >tol) //Check if the difference is in the tolerance else change horizontal angle
  {
  if (avl > avr)
  {
   servoh = –servoh;
   if (servoh < 0)
   {
   servoh = 0;
   }
  }
  else if (avl < avr)
  {
   servoh = ++servoh;
   if (servoh > 180)
   {
   servoh = 180;
   }
  }
  else if (avl = avr)
  {
   // nothing
  }
  horizontal.write(servoh);
  }
   delay(dtime);
}
```

Figure A.1. Tracking control C++ program (continued).

- *Compute the mean values (means):* Compute the mean values for each couple of LDRs among the following four sensors (Figure 13).
  - Between LDR1 and LDR3 ⟶ Mean value of the up side,
  - Between LDR2 and LDR4 ⟶ Mean value of the low side,
  - Between LDR1 and LDR2 ⟶ Mean value of the left side,
  - Between LDR3 and LDR4 ⟶ Mean value of the right side.
- *Compute the difference values (Diffs):*
  - Compute the difference between the mean value of the up and down sides to control the vertical motor;
  - Compute the difference between the mean value of the left and right sides to control the horizontal motor.
- $-1 * tol > dvert \| dvert > tol$: The previous obtained result ≪Compute diffs≫ will be compared to tolerance input signal (tol.). If we obtain an equal value, the motor is at rest; otherwise, if we have a different value, the motor will move to change the vertical angle.
- *meanh > meanl; (h: high; l: low):* Accordingly, the values of the vertical allow for the correction of the vertical system position. The motor will move the panel toward the side where there is a big value; however, when the reached angle is 180° or 0°, the motor stops;
- $-1 * tol > dhoriz \| dhoriz > tol$: The previous obtained result ≪Compute diffs≫ will be compared to tolerance input signal (tol.). If we obtain an equal value, the motor is at rest; otherwise, if we have a different value, the motor will move to change horizontal angle;
- *meanl > meanr; (l: left; r: right):* Accordingly, the values of the horizontal allow for the correction of the horizontal system position. The motor will move the panel toward the side where there is a big value; however, when reached angle is 180° or 0°, the motor stops;

The PV system needs two different pauses: The short pause is the delay of the position of the PV Panel relative to the sun ray. We can fix a delay of

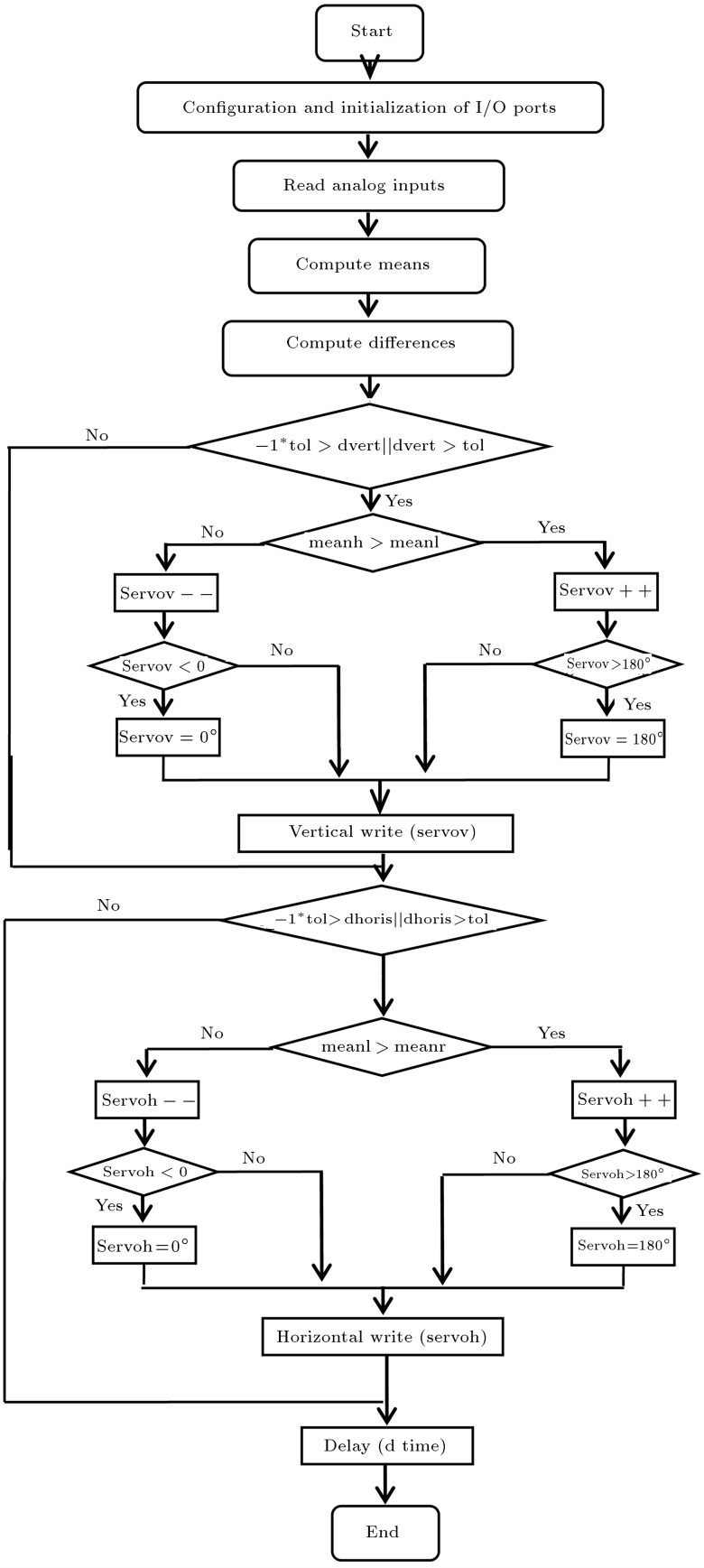

Figure B.1. Tracking control flowchart.

30 minutes to avoid wasting of energy, after which the panel changes the inclination of 9 or 10 degrees following the new position of the sun.

The long mean pause of 12 h (from 10 h to 15 h depending on the season) will be at the end of the day, permitting panels to have their initial positions.

Biographies

Abdelhamid Mansouri was born in Sidi-Okba, Algeria in 1951. He received the DES (Diploma of Higher Studies) degree from the University of Algiers in 1979 and the MPhil degree in Electrical Engineering from the University of Sétif in 1996. He was an Assistant Lecturer at the Department of Physics, University of Annaba in 1979, and was an Electrical Engineer in Industrial Societies Enageo & Elatex from 1981 to 1983. Currently, he is a Lecturer at the Department of Electrical Engineering, University of Sétif-1, where he has been since 1983. Being a member of laboratory of power electronics and industrial control (LEPCI), his research interests are in the areas of identification and optimal control of electrical machines, artificial intelligence techniques, and renewable energies.

Fateh Krim received BSc degree from Claude Bernard University of Lyon, France in 1976, MSc and Engineer degrees in Electrical Engineering from Ecole Centrale, Lyon in 1979, the PhD from Polytechnic National Institute of Grenoble, France, and the special doctorate from University of Sétif, Algeria in 1982 and 1996, respectively. From 1982 to 1985, he was the Head of IC design Department at CIT-Alcatel, Paris, France. He is currently a Professor of Electrical Engineering at University of Sétif-1, Algeria and Director of laboratory of Power Electronics and Industrial Electronics. His main research interests are systems control, power and industrial electronics, renewable energies. In these fields, he has more than 80 papers in international journals and refereed conference proceedings. He is a reviewer in 13 journals. Professor Fateh Krim is a senior IEEE member and a member of IEEE Industrial Electronics Society, IEEE Power Electronics Society, IEEE Power Engineering Society, and IEEE Computational Intelligence Society. He is the President of IEEE Algeria Section and industrial electronics and industry applications chapter.

Zakaria Khouni was born in Sétif, Algeria in 1988. He received his Bachelor degree in Electrical Engineering (EEA) and his master's degree in Industrial Electronics from Ferhat Abbas Sétif-1 University, Sétif, Algeria in 2012 and 2014, respectively. He is currently pursuing his PhD at the Electronics Department at Sétif-1 University's, LCCNS Laboratory. His research interests include embedded system technologies, fuzzy logic systems, DSP system, and FPGA cards.